ISSN 1070-3284, Russian Journal of Coordination Chemistry, 2017, Vol. 43, No. 12, pp. 858–863. © Pleiades Publishing, Ltd., 2017.
Original Russian Text © G.K. Fukin, M.A. Samsonov, E.V. Baranov, A.I. Poddel'skii, V.K. Cherkasov, 2017, published in Koordinatsionnaya Khimiya, 2017, Vol. 43, No. 12, pp. 759–764.

# Electron Density Distribution in Crystals of the Antimony(V) Spiroendoperoxide Complexes

**G. K. Fukin*, M. A. Samsonov, E. V. Baranov, A. I. Poddel'skii, and V. K. Cherkasov**

*Razuvaev Institute of Organometallic Chemistry, Russian Academy of Sciences, ul. Tropinina 49, Nizhny Novgorod, 603600 Russia*

**e-mail: gera@iomc.ras.ru*

Received July 6, 2017

**Abstract**—The experimental and theoretical electron densities in complexes [6-(2,6-di-*iso*-propylphenyl)imino-2,4-di-*tert*-butylcyclohexa-2,4-diene-1-peroxo-1-olato-*N*,*O*,*O*']tris(*p*-chlorophenyl)antimony(V), (*p*-Cl–$C_6H_4)_3$Sb(2,6-*iso*-Pr–Ph–AP) · $O_2$ (**I**), and [6-(2,6-dimethylphenyl)imino-2,4-di-*tert*-butylcyclohexa-2,4-diene-1-peroxo-1-olato-*N*,*O*,*O*']tris(*p*-chlorophenyl)antimony(V), (*p*-Cl–$C_6H_4)_3$Sb(2,6-Me–Ph–AP) · $O_2$ (**II**), where AP is 4,6-di-*tert*-butyl-*N*-*o*-iminobenzoquinone dianion, are studied on the basis of high-resolution X-ray diffraction data and theoretical calculations using the density functional theory (B3LYP/DGDZVP). The nature of chemical bonds and the charge distribution on atoms are studied, and the energy of molecular oxygen addition to the Sb(V) *o*-aminophenolate complexes is estimated. The structures are deposited with the Cambridge Crystallographic Data Centre (CIF files CCDC nos. 1560600 (spherical refinement) and 1560601 (multipole refinement) for complex **I**; 1560602 (spherical) and 1560603 (multipole) for complex **II**).

*Keywords*: spiroendoperoxide complexes of Sb(V), high-resolution X-ray diffraction studies, DFT calculations, R. Bader's theory "Atoms in Molecules"

**DOI:** 10.1134/S1070328417120028

## INTRODUCTION

The spiroendoperoxide complexes of antimony(V) are the addition products of molecular oxygen to the Sb(V) catecholate and amidophenolate complexes [1, 2]. The addition is reversible. The electronic (energies of higher occupied molecular orbitals and ionizations) and steric criteria were found for the Sb(V) catecholate and *o*-amidophenolate complexes [3–5], and they allow one to explain reasonably this phenomenon and predict the activity (inertness) of these complexes toward $O_2$. In addition, the electron density topology was studied for a series of the catecholate [3] and *o*-amidophenolate [6] complexes of antimony(V). In turn, these data are absent for the spiroendoperoxide complexes. Therefore, it seems important to study the electron density topology, the nature of chemical bonds, and the charge distribution in the Sb(V) spiroendoperoxide complexes and to find changes in the topological characteristics of the electron density compared to those of the antimony(V) *o*-amidophenolate complexes.

## EXPERIMENTAL

The spiroendoperoxide complexes of Sb(V), (*p*-Cl–$C_6H_4)_3$Sb(2,6-$^i$Pr–Ph–AP) · $O_2$ (**I**) and (*p*-Cl–$C_6H_4)_3$Sb(2,6-Me–Ph–AP) · $O_2$ (**II**), were synthesized using known procedures [1, 2].

High-resolution X-ray diffraction studies for complexes **I** and **II** were carried out on a SMART APEX I automated diffractometer (graphite monochromator, Mo$K_\alpha$ radiation, $\lambda = 0.71073$ Å) at 100 K. Experimental data of intensities were integrated using the SAINT program [7]. Absorption corrections were applied using the SADABS program [8]. The structures were solved by a direct method and refined by full-matrix least squares for $F^2$ (SHELXTL) [9]. All non-hydrogen atoms were refined anisotropically. Hydrogen atoms were placed in the geometrically calculated positions and refined in the riding model. The solvate acetone molecule in the common position was found in complex **I**. The site occupancies of the atoms of this molecule are 0.125.

The multiple refinement was carried out within the Hansen–Coppens formalism [10] using the MoPro program package [11]. Before the refinement C–H bond distances in the high-resolution X-ray diffraction studies were normalized to the values obtained in neutron diffraction analyses. [12]. The level of the multipole expansion was hexadecapole for antimony atoms, octupole for all other non-hydrogen atoms and one dipole for hydrogen atoms. The solvate acetone molecule was not involved in the multipole refine-

**Table 1.** Selected crystallographic characteristics and the high-resolution X-ray diffraction experimental parameters for complexes **I** and **II**

| Parameter | Value | |
|---|---|---|
| | **I** | **II** |
| Empirical formula | $C_{44.4}H_{49.8}Cl_3NO_{3.1}Sb$ | $C_{40}H_{41}Cl_3NO_3Sb$ |
| *FW* | 875.211 | 811.847 |
| *T*, K | 100(2) | 100(2) |
| Crystal system | Monoclinic | Monoclinic |
| Space group | *C*2/*c* | *C*2/*c* |
| *a*, Å | 28.2093(3) | 34.9557(5) |
| *b*, Å | 15.5003(2) | 12.8592(2) |
| *c*, Å | 23.0621(3) | 17.8266(3) |
| β, deg | 118.536(1) | 111.253(1) |
| *V*, Å$^3$ | 8858.93(19) | 7468.1(2) |
| *Z* | 8 | 8 |
| $\rho_{calc}$, g cm$^{-3}$ | 1.313 | 1.445 |
| μ, mm$^{-1}$ | 0.841 | 0.992 |
| *F*(000) | 3600 | 3312 |
| Crystal size, mm | 0.39 × 0.28 × 0.28 | 0.41 × 0.21 × 0.17 |
| Range of θ, deg | 1.55–51.42 | 1.70–51.43 |
| Number of collected/independent reflections | 368074/38797 | 399238/30655 |
| $R_1$, $wR_2$ ($I > 2\sigma(I)$) | 0.0293, 0.0213 | 0.0272, 0.0200 |
| Goodness-of-fit | 0.991 | 0.991 |
| $\Delta\rho_{max}/\Delta\rho_{min}$, *e* Å$^{-3}$ | 1.115/–0.387 | 0.379/–0.187 |

ment. All bonded pairs of atoms satisfy the Hirshfeld rigid-bond criteria [13]. The topological analysis of the experimental function ρ(*r*) was performed using the WINXPRO program package [14].

Quantum-chemical calculations were performed by the B3LYP/DGDZVP (functional/basis set) density functional method using the Gaussian 03W program [15]. The absence of imaginary frequencies indicates that the molecules are at the potential energy minimum. The topological analysis of the theoretical function ρ(*r*) was performed using the AIMALL program package [16].

The main crystallographic characteristics and X-ray diffraction experimental parameters for complexes **I** and **II** are presented in Table 1. The structures were deposited with the Cambridge Crystallographic Data Centre (CIF files CCDC nos. 1560600 (spherical refinement) and 1560601 (multipole) for complex **I**, 1560602 (spherical refinement) and 1560603 (multipole) for complex **II**; deposit@ccdc.cam.ac.uk or http://www.ccdc.cam.ac.uk/data_request/cif).

## RESULTS AND DISCUSSION

The final products of molecular oxygen addition to the antimony catecholate and *o*-amidophenolate complexes are the spiroendoperoxide derivatives [1, 2]. The reversible addition of molecular oxygen to the Sb(V) catecholate (X = O) and *o*-amidophenolate (X = N–Ar) complexes is presented in the scheme.

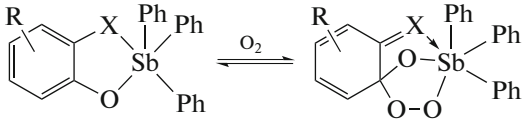


According to the X-ray diffraction data, the coordination environment of the Sb(V) atoms in spiroendoperoxide complexes **I** and **II** are a distorted octahedron (Fig. 1). The Sb(1)–O(1) and Sb(1)–O(2) bond lengths are 2.0237(1), 2.0624(2) Å in complex **I** and 2.0257(6), 2.0678(6) Å in complex **II**. The Sb(1)–N(1) distances (2.4776(6) Å in **I** and 2.5539(6) Å in **II**) differ noticeably. Note that the Sb(1)–N(1) bond lengths also differ noticeably according to the earlier published data [1, 2] on the structures of the Sb(V)

spiroendoperoxide complexes (2.425(3) Å in $(C_6H_5)_3Sb(2,6\text{-}^iPr{-}Ph{-}AP) \cdot O_2$ and 2.4802(14) Å in $(C_6H_5)_3Sb(2,6\text{-}Me{-}Ph{-}AP) \cdot O_2$). The Sb(1)–C(Ph) distances (2.1345(8)–2.1382(7) Å in **I** and 2.1330(8)–2.1426(8) Å in **II**) are close to each other. The O(2)–O(3) distances in the added oxygen molecule are 1.4590(9) Å in complex **I** and 1.4603(9) Å in complex **II** and are close to similar bond lengths in the earlier reported complexes (1.461(3)–1.475(2) Å) [1, 2]. On the whole, the geometric characteristics of complexes **I** and **II** are consistent with similar characteristics for the antimony catecholate ($(C_6H_5)_3Sb(3,6\text{-}^tBu\text{-}4\text{-}OMe{-}Cat) \cdot O_2$ and $(C_6H_5)_3Sb(3,6\text{-}^tBu{-}4,5\text{-}OMe{-}Cat) \cdot O_2$), where Cat is *o*-benzoquinone dianion, and *o*-amidophenolate ($(C_6H_5)_3Sb(2,6\text{-}^iPr{-}Ph{-}AP) \cdot O_2$, $(C_6H_5)_3Sb(2,6\text{-}Me{-}Ph{-}AP) \cdot O_2$) spiroendoperoxide compounds [1, 2]. It is important that a noticeable shortening of the Sb(1)–O(1) bond is observed in spiroendoperoxide complexes **I** (to 2.0237(5) Å), **II** (to 2.0257(6) Å), $(C_6H_5)_3Sb(2,6\text{-}^iPr{-}Ph{-}AP) \cdot O_2$ (to 2.032(2) Å), and $(C_6H_5)_3Sb(2,6\text{-}Me{-}Ph{-}AP) \cdot O_2$ (to 2.024(1) Å) compared to the *o*-amidophenolate complexes $(cyclohex)_3Sb(2,6\text{-}^iPr{-}Ph{-}AP)$ (2.1162(5) Å) and $(p\text{-}F{-}Ph)_3Sb(2,6\text{-}Me{-}Ph{-}AP)$ (2.0685(13) Å) [6].

The distribution of the deformation electron density around the Sb atom in spiroendoperoxide complexes **I** and **II** is shown in Fig. 2. The maxima of the deformation electron density on the Sb(1)–O(1) and Sb(1)–N(1) bonds are appreciably shifted to the O(1) and N(1) atoms. The maxima of the deformation electron density on N(1)–C(2) and O(1)–C(1) bonds are located almost at the middle of the bonds in complexes **I** and **II**. Interestingly, a substantial depletion of the deformation electron density between the oxygen atoms is observed on the O(2)–O(3) bond (Figs. 3b, 3d).

According to Bader's theory [17], the Sb–O, Sb–C, O–O, and Sb–N bonds are classified as intermediate interactions ($\nabla^2\rho(r) > 0$, $h_e(r) < 0$), whereas O–C, N–C, and C–C are shared ($\nabla^2\rho(r) < 0$, $h_e(r) < 0$) (Table 2). The quantum-chemical calculations of the isolated molecules adequately reproduce the geometric and topological characteristics of complexes **I** and **II** in the crystalline state. It should be mentioned that the values of $\rho(r)$ at the critical point (3, −1) (CP(3, −1)) at the Sb(1)–N(1) bond in spiroendoperoxide complexes **I** (0.057 a.u.) and **II** (0.045 a.u.) decrease almost two times compared to those for the *o*-amidophenolate complexes $(cyclohex)_3Sb(2,6\text{-}^iPr{-}Ph{-}AP)$ (0.117 a.u.) and $(p\text{-}F{-}Ph)_3Sb(2,6\text{-}Me{-}Ph{-}AP)$ (0.112 a.u.) [6]. However, no changes in the chemical binding type occur. The values of $\rho(r)$ at the CP(3, −1) on the Sb(1)–O(1) and O(1)–C(1) bonds in complexes **I** and **II** are 0.115, 0.291 and 0.110, 0.325 a.u., respectively. This is comparable with similar values of

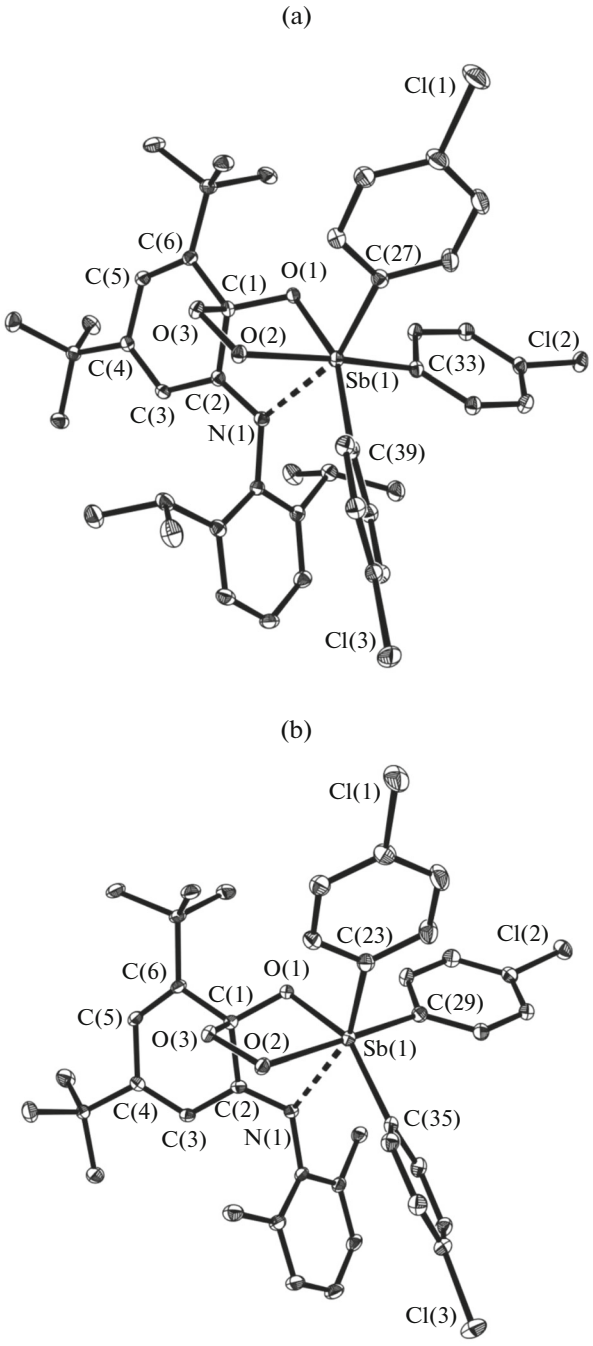


**Fig. 1.** Molecular structures of complexes (a) **I** and (b) **II**. Thermal ellipsoids are presented with 30% probability. Hydrogen atoms and solvent molecules are omitted.

$\rho(r)$ for the Sb(1)–O(1) and O(1)–C(1) bonds in the $(cyclohex)_3Sb(2,6\text{-}^iPr{-}Ph{-}AP)$ (0.103 and 0.325 a.u., respectively) and $(p\text{-}F{-}Ph)_3Sb(2,6\text{-}Me{-}Ph{-}AP)$ (0.077 and 0.308 a.u., respectively) complexes [6]. The values of $\rho(r)$ at the CP(3, −1) for the Sb–C(Ph) bonds are similar (0.094–0.117 a.u. for **I** and **II**) and comparable with those in the antimony(V) *o*-amidophenolate complexes (0.094–0.108 a.u.). In spite of

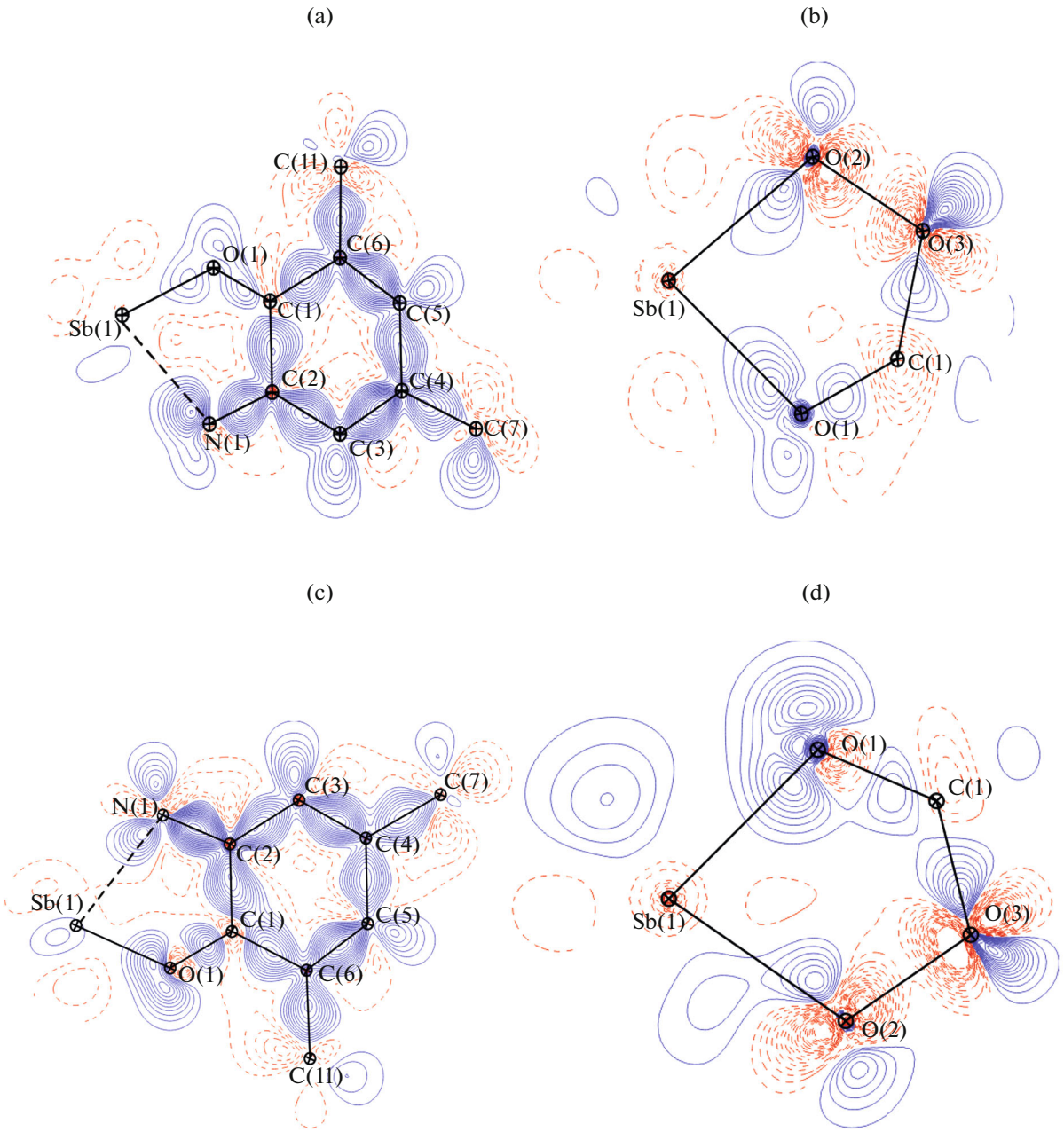


**Fig. 2.** Sections of the deformation electron density in complexes (a, b) **I** and (c, d) **II** in the planes (a, c) C(2)C(4)C(6) and (b, d) Sb(1)O(1)O(3). Solid isolines show the concentration of the deformation electron density, and dashed lines show depletion ($\pm 0.05\ e\ Å^{-3}$).

the fact that the deformation electron density distribution indicates a substantial depletion of the electron density on the O(2)–O(3) bond (added oxygen molecule) in complexes **I** and **II**, the values of $\rho(r)$ at the CP(3, –1) (0.247 and 0.230 a.u., respectively) on these bonds are close to similar characteristics for the shared O(3)–C(1) interactions (0.241 and 0.230 a.u., respectively).

The energies for the Sb(1)–O(1) and Sb(1)–O(2) bonds were estimated according to the Espinosa equation [18]. The energies of these bonds are –57.73, –51.77 kcal/mol in complex **I** and –55.53, –49.26 kcal/mol in complex **II**. Note that they appreciably exceed the energies of the Sb(1)–N(1) bonds in complexes **I** (–16.63 kcal/mol) and **II** (–11.92 kcal/mol). The difference between the total energies of the final spiroendoperoxide complexes **I** and **II** and the starting substances (*o*-amidophenolate complex and molecular oxygen) was determined by the DFT calculations (B3LYP/DGDZVP) of the

**Table 2.** Selected bond lengths and topological parameters at the CP(3, −1) for the ($p$-Cl–$C_6H_4$)$_3$Sb(2,6-$^i$Pr–Ph–AP) · $O_2$ (**I**) and ($p$-Cl–$C_6H_4$)$_3$Sb(2,6-Me–Ph–AP) · $O_2$ (**II**) complexes according to the high-resolution data and DFT calculations*

| Bond | Distance, Å | ν($r$), a.u. | ρ($r$), a.u. | $\nabla^2\rho(r)$, a.u. | $h_e(r)$, a.u. |
|---|---|---|---|---|---|
| | | | **I** | | |
| Sb(1)–O(1) | 2.0237(5) | −0.184 | 0.115 | 0.311 | −0.053 |
| | (2.08247) | (−0.137) | (0.094) | (0.294) | (−0.032) |
| Sb(1)–O(2) | 2.0624(6) | −0.165 | 0.109 | 0.270 | −0.049 |
| | (2.12211) | (−0.121) | (0.089) | (0.254) | (−0.030) |
| Sb(1)···N(1) | 2.4776(6) | −0.053 | 0.057 | 0.058 | −0.019 |
| | (2.52978) | (−0.037) | (0.044) | (0.092) | (−0.007) |
| Sb(1)–C(27) | 2.1345(8) | −0.150 | 0.109 | 0.091 | −0.064 |
| | (2.17178) | (−0.113) | (0.106) | (0.062) | (−0.049) |
| Sb(1)–C(33) | 2.1370(7) | −0.162 | 0.112 | 0.136 | −0.064 |
| | (2.18173) | (−0.109) | (0.104) | (0.063) | (−0.047) |
| Sb(1)–C(39) | 2.1382(7) | −0.148 | 0.107 | 0.100 | −0.061 |
| | (2.17568) | (−0.110) | (0.105) | (0.063) | (−0.047) |
| O(1)–C(1) | 1.3651(9) | −0.682 | 0.291 | −0.702 | −0.426 |
| | (1.37269) | (−0.610) | (0.289) | (−0.562) | (−0.375) |
| O(3)–C(1) | 1.4704(9) | −0.516 | 0.241 | −0.250 | −0.289 |
| | (1.47703) | (−0.390) | (0.236) | (−0.446) | (−0.251) |
| O(2)–O(3) | 1.4590(9) | −0.618 | 0.247 | 0.710 | −0.220 |
| | (1.45420) | (−0.345) | (0.265) | (0.231) | (−0.144) |
| N(1)–C(2) | 1.2927(9) | −0.988 | 0.368 | −1.147 | −0.637 |
| | (1.30035) | (−0.824) | (0.351) | (−0.685) | (−0.497) |
| N(1)–C(15) | 1.4313(10) | −0.651 | 0.282 | −0.535 | −0.392 |
| | (1.44040) | (−0.434) | (0.268) | (−0.636) | (−0.297) |
| C(1)–C(2) | 1.5362(10) | −0.529 | 0.250 | −0.502 | −0.327 |
| | (1.54325) | (−0.263) | (0.249) | (−0.632) | (−0.211) |
| | | | **II** | | |
| Sb(1)–O(1) | 2.0257(6) | −0.177 | 0.110 | 0.375 | −0.042 |
| | (2.08552) | (−0.136) | (0.094) | (0.290) | (−0.032) |
| Sb(1)–O(2) | 2.0678(6) | −0.157 | 0.106 | 0.237 | −0.049 |
| | (2.12090) | (−0.122) | (0.089) | (0.255) | (−0.029) |
| Sb(1)···N(1) | 2.5539(7) | −0.038 | 0.045 | 0.063 | −0.011 |
| | (2.52354) | (−0.037) | (0.044) | (0.094) | (−0.007) |
| Sb(1)–C(23) | 2.1384(8) | −0.133 | 0.100 | 0.124 | −0.051 |
| | (2.17109) | (−0.113) | (0.106) | (0.062) | (−0.049) |
| Sb(1)–C(29) | 2.1426(8) | −0.162 | 0.117 | 0.010 | −0.080 |
| | (2.17740) | (−0.111) | (0.104) | (0.064) | (−0.047) |
| Sb(1)–C(35) | 2.1330(8) | −0.129 | 0.094 | 0.210 | −0.038 |
| | (2.17463) | (−0.111) | (0.105) | (0.063) | (−0.048) |
| O(1)–C(1) | 1.3678(9) | −0.826 | 0.325 | −0.675 | −0.498 |
| | (1.37339) | (−0.609) | (0.289) | (−0.564) | (−0.374) |
| O(3)–C(1) | 1.469(1) | −0.482 | 0.230 | −0.190 | −0.265 |
| | (1.47680) | (−0.390) | (0.236) | (−0.446) | (−0.251) |
| O(2)–O(3) | 1.4603(9) | −0.640 | 0.254 | 0.657 | −0.238 |
| | (1.45352) | (−0.346) | (0.265) | (0.230) | (−0.144) |
| N(1)–C(2) | 1.2945(9) | −1.196 | 0.416 | −1.640 | −0.803 |
| | (1.29926) | (−0.828) | (0.352) | (−0.682) | (−0.499) |
| N(1)–C(15) | 1.4246(9) | −0.659 | 0.289 | −0.800 | −0.429 |
| | (1.43552) | (−0.444) | (0.270) | (−0.641) | (−0.302) |
| C(1)–C(2) | 1.5292(9) | −0.603 | 0.272 | −0.630 | −0.380 |
| | (1.54296) | (−0.263) | (0.250) | (−0.632) | (−0.211) |

* The distances and topological parameters given without parentheses were obtained from the high-resolution experimental data, and the values in parentheses were obtained from the DFT calculations.

**Table 3.** Atomic charges in complexes **I** and **II***

| Complex | AIM charges, e | | | | | | |
|---|---|---|---|---|---|---|---|
| | Sb(1) | O(1) | O(2) | O(3) | N(1) | C(1) | C(2) |
| **I** | 1.39 (2.30) | −0.89 (−1.16) | −0.60 (−0.61) | −0.46 (−0.50) | −0.95 (−1.19) | 0.89 (0.95) | 0.61 (0.60) |
| **II** | 1.57 (2.30) | −1.06 (−1.16) | −0.59 (−0.62) | −0.38 (−0.50) | −1.19 (−1.20) | 0.72 (0.95) | 0.79 (0.61) |

* The charges presented without parentheses were obtained from the high-resolution experimental data, and the charges in parentheses were obtained from the DFT calculations. The charges were calculated in terms of R. Bader's theory "Atoms in Molecules."

isolated molecules. These values are the energies of molecular oxygen addition to the corresponding Sb(V) *o*-amidophenolate complexes and are equal to −10.06 kcal/mol for complex **I** and −8.60 kcal/mol in complex **II**. It is important that the obtained values of energy are well consistent with the experimental values of enthalpy of molecular oxygen elimination for the related $(C_6H_5)_3Sb(2,6-^iPr-Ph-AP) \cdot O_2$ (9.1 ± 0.5 kcal/mol) and $(C_6H_5)_3Sb(2,6\text{-}Me-Ph-AP) \cdot O_2$ (9.6 ± 0.5 kcal/mol) spiroendoperoxide complexes [19].

The experimental charges on the Sb(1) atoms are 1.39*e* and 1.57*e* in complexes **I** and **II**, respectively (Table 3), which are substantially lower than those in the *o*-amidophenolate complex $(p\text{-}F-Ph)_3Sb(2,6\text{-}Me-Ph-AP)$ (2.46*e*), where the fluorine atom is located as halogen in the *p*-position of the phenyl ring [6]. A comparison of the charges in spiroendoperoxide (**I** and **II**) and *o*-amidophenolate ($(cyclohex)_3Sb(2,6\text{-}^iPr-Ph-AP)$ and $(p\text{-}F-Ph)_3Sb(2,6\text{-}Me-Ph-AP)$) complexes [6] shows that the addition of $O_2$ substantially changes the charges on the C(2) atoms. The experimental charges on the C(2) atoms in the *o*-amidophenolate complexes are 0.16*e* and 0.35*e* and are substantially less positive than similar charges in spiroendoperoxide complexes **I** and **II**. Evidently, the addition of molecular $O_2$ to the Sb(1) and O(1) atoms does not change the atomic environment around the C(2) atoms but exerts a substantial effect on the surrounding distances compared to those in the Sb(V) *o*-amidophenolate complexes. This results in a change in the multiplicities (orders) of the bonds around the C(2) atoms and, as a consequence, decreases the electron density in the corresponding atomic basin.

## ACKNOWLEDGMENTS

This work was supported by the Russian Foundation for Basic Research, projects nos. 16-33-00117, 17-03-01257, and 15-43-02170r_povolzh'e_a.

## REFERENCES

1. Abakumov, G.A., Poddel'sky, A.I., Grunova, E.V., et al., *Angew. Chem., Int. Ed. Engl.*, 2005, vol. 44, p. 2767.
2. Cherkasov, V.K., Abakumov, G.A., Grunova, E.V., et al., *Chem.-Eur. J.*, 2006, vol. 12, p. 3916.
3. Fukin, G.K., Baranov, E.V., Jelsch, C., et al., *J. Phys. Chem. A*, 2011, vol. 115, p. 8271.
4. Fukin, G.K., Baranov, E.V., Poddel'sky, A.I., et al., *ChemPhysChem*, 2012, vol. 13, p. 3773.
5. Fukin, G.K., Samsonov, M.A., Poddel'skii, A.I., and Cherkasov, V.K., *Izv. Akad. Nauk, Ser. Khim.*, 2016, vol. 1, p. 61.
6. Fukin, G.K., Samsonov, M.A., Baranov, E.V., et al., *Izv. Akad. Nauk, Ser. Khim.*, 2016, vol. 1, p. 54.
7. *SAINT. Version 8.27B. Data Reduction and Correction Program*, Madison: Bruker AXS, 2014.
8. Sheldrick, G.M. *SADABS. Version 2014/5. Bruker/Siemens Area Detector Absorption Correction Program*, Madison: Bruker AXS, 2014.
9. Sheldrick G.M., *SHELXTL. Version 2008/4. Structure Determination Software Suite*, Madison: Bruker AXS, 2000.
10. Hansen, N.K. and Coppens, P., *Acta Crystallogr., Sect. A: Cryst. Phys., Diffr., Theor. Gen. Crystallogr.*, 1978, vol. 34, p. 909.
11. Jelsch, C., Guillot, B., Lagoutte, A., and Lecomte, C., *J. Appl. Crystallogr.*, 2005, vol. 38, p. 38.
12. Allen, F.H., Kennard, O., Watson, D.G., et al., *J. Chem. Soc., Perkin Trans.*, 1987, vol. 2, p. 1.
13. Hirshfeld, F.L., *Acta Crystallogr., Sect. A: Cryst. Phys., Diffr., Theor. Gen. Crystallogr.*, 1976, vol. 32, p. 239.
14. Stash, A. and Tsirelson, V., *J. Appl. Crystallogr.*, 2002, vol. 35, p. 371.
15. Frisch, M.J., Trucks, G.W., Schlegel, H.B., et al., *Gaussian 03. Kevision C.02*, Wallingford: Gaussian, Inc., 2004.
16. Keith, T.A., *AIMAll (version 14.06.21). TK Gristmill Software*, Overland Park KS, 2014. hhtp://aim.tkgristmill.com.
17. Bader, R.F.W., *Atoms in Molecules: A Quantum Theory*, Oxford: Oxford Univ., 1990.
18. Espinosa, E., Molins, E., and Lecomte, C., *Chem. Phys. Lett.*, 1998, vol. 285, p. 170.
19. Poddel'skii, A.I., Antimony(V) complexes with redox active catecholate and *o*-amidophenolate ligands. reversible addition of molecular oxygen, *Doctoral (Chem.) Dissertation*, Nizhny Novgorod: Lobachevsky Nizhny Novgorod State University, 2013.

*Translated by E. Yablonskaya*